International Journal of Research in Pharmacy and Pharmaceutical Sciences
ISSN: 2455-698X
Impact Factor: RJIF 5.22
www.pharmacyjournal.in
Volume 3; Issue 2; March 2018; Page No. 119-122

Silver nanoparticle/MWCNT Modified Screen Printed Electrode for the detection of Hydrazine

Gita Rani[1*], Neelam[2], Mukesh Kumar[3]
[1, 2] Department of Chemistry, Chaudhary Devi Lal University, Sirsa, Haryana, India
[3] Department of Education O/o District Education Officer, Sirsa, Haryana, India

Abstract
This article deals with the synthesis of silver oxide nanoparticles by coprecipitation method. The modified screen printed electrode shows the determination of hydrazine in food samples. The crystalline size, surface morphology and optical properties of prepared silver oxide nanoparticles has been investigated by XRD, SEM and FTIR techniques. Under the experimental conditions, the hydrazine concentration has been obtained in the range of 5-50 µM, good sensitivity of 97.8 µA $\mu M^{-1}cm^{-2}$ and low detection limit 5µM and long term stability. The cyclic voltammetry and Chronoamperometry studies show the electrochemical performance towards the oxidation of hydrazine.

Keywords: silver oxide nanoparticles, Co-precipitation method, XRD, SEM, Optical properties

1. Introduction
Hydrazine (N_2H_4) is a small inorganic water soluble molecule. It is a colorless liquid having molecular weight of 32 g/mol [1]. It has been widely used in military, industrial, corrosion inhibitor, pesticides and plant growth regulators [2]. Hydrazine is a toxic material that has carcinogenic and hepatotoxic effect and can be easily absorbed by human body. If hydrazine is introduced or inhaled by living organisms, its kidney, lungs, central nervous system and liver can be injured. A dangerous effect is observed on the reproductive system of animals and specially decreased the size of testes and ovary and the production of sperms [3]. Due to above reasons there is need to develop a sensitive, fast and reliable analytical tool for the effective detection of hydrazine [4]. There are several methods available for the detection of hydrazine pesticide like Atomic Absorption Spectrophotometer (AAS), Flow Injection Analysis (FIA), Surface-Enhanced Raman Spectroscopy (SERS) [5], Gas Chromatography-Mass Spectroscopy (GC-MS) [6, 7, 8], Liquid Chromatography-Mass Spectroscopy (LC-MS) [9]. All these methods have their own limitations and are time consuming. Among these methods, electroanalytical have attracted attention due to their sensitivity, selectivity, portability and low cost [10, 11, 12].
The important key in the electrode modification is the material with good electrical conductivity and better electrocatalysis. Nanoparticles and carbon nanotubes are used in a variety of electrocatalyst applications because of good conductivity, high stability and fast electron transfer. Among many nanoparticles have unique optical [13, 14], electrical [15, 16, 17], catalytic [18, 19, 20] and antibacterial properties [21, 22]. In this work we synthesize an AgO/MWCNT modified screen printed electrode based electrochemical sensor for the detection of hydrazine as pesticide.

2. Experimental
2.1 Materials
Silver nitrate ($AgNO_3$) was purchased from Qualigens. Potassium chloride (KCl), sodium phosphate monobasic (NaH_2PO_4), sodium phosphate dibasic (Na_2HPO_4), potassium ferrocyanide K_4 [$Fe(CN)_6$], potassium ferricyanide K_3 [$Fe(CN)_6$], sodium chloride (NaCl), multiwalled carbon nanotube (MWCNT) were purchased from CDH, New Delhi. All others chemicals were of analytical grade and used without further purification. The stock solutions of hydrazine were freshly prepared in phosphate buffer (pH 7.0).

2.2 Synthesis of AgO nanoparticles
AgO nanoparticles were prepared by coprecipitation method. In this method, 0.1 M $AgNO_3$ solution was prepared in double de-ionized water with continuous stirring to get a homogeneous solution. 0.1 M sodium hydroxide solution was added dropwise into the above solution with continuous stirring for 3 hrs. The resultant precipitates thus obtained were washed with double distilled water and after acetone. Precipitates were dried at 100 ^oC in oven for 5 hrs. Finally these were put into muffle furnace at 600 ^oC for 2 hrs and silver oxide nanoparticles were formed.

2.3 Fabrication of AgO/CNT modified screen printed carbon electrode
Carbon nanotubes (CNT), nanoparticles (NP) and gluteraldehyde were prepared by mixing in the ratio 5:3:2. Mix the above solution vigorously to get a homogeneous mixture. The above solution was then used for the fabrication process of the screen printed carbon electrode. The dot of SPCE i.e. working electrode was filled with above slurry using the pipette. Then the electrode was dried in the microwave oven at 70 ^oC for 5 minutes and left at room temperature for 24 hrs for the fixation of slurry on the working electrode dot of SPCE.

2.4 Characterization
The crystalline size of AgO nanoparticles was investigated by using X-ray diffraction (XRD) pattern, using D-8 Advance,

Bruker diffraction, with monochromatic Cu Kα radiation (λ = 1.5418 Å). Scanning electron microscope (SEM) analysis was done through Hitachi S3700 SEM using an acceleration of 15 KV. The size of nanoparticles are calculated by SEM. The cyclic voltammetry (CV) and chronoamperometry (CA) studies have been done using an Autolab Potentiostat/ Galvanostat (Metrohm). The electrochemical measurements have been conducted on a three-electrode system using AgO/CNT/SPCE as the working electrode, a platinum (Pt) wire as the counter and saturated Ag/AgCl as a reference electrode in a phosphate buffer saline (PBS, pH 7.0,NaCl) containing 5 mM $[Fe(CN)_6]^{3-/-4}$ as a mediator.

3. Results and discussion

3.1 XRD analysis

The X-ray diffraction pattern revealed the major peaks at 2θ values of 32.16 (111), 37.31 (200), 53.79 (220), 64.07 (311) respectively. The lattice constant of a = 4.816 which is confirmed by JCPDS card no. 76-1489. Therefore the synthesized sample is AgO nanoparticles. Average particle size was found to be 29 nm using Debye Scherrer formula (D = 0.9 λ/ β cos θ),

Where D is the crystallite size, λ is the X-ray wavelength (1.5406 Å), θ is the Bragg diffraction angle, β is the full width at half maximum of the diffraction peak.

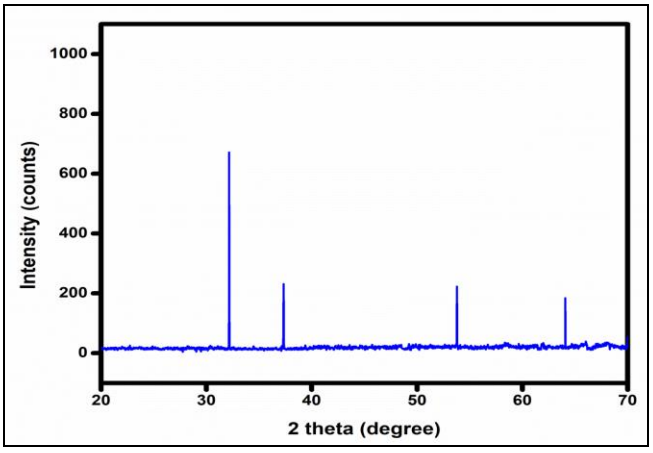

Fig 1: XRD spectra of silver oxide NPs

3.2 SEM analysis

The surface morphology of synthesized silver oxide NPs shows the magnification of 50 µm. The silver oxide nanoparticles are crystalline in nature and 20-70 nm in size.

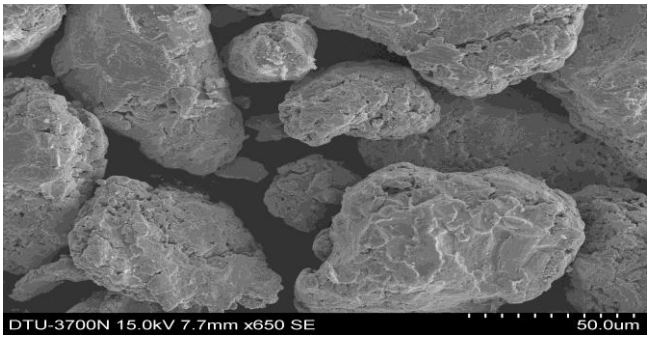

Fig 2: XRD spectra of silver oxide NPs

3.3 FTIR Spectroscopy

Figure 3 shows the FTIR spectra of silver oxide nanoparticles by co-precipitation method. Various peaks are observed at different regions of FTIR spectrum. The absorption band at 3457 and 1646 $cm^{-1}$are ascribed to stretching and bending vibration of –OH respectively. Further peaks at 2923 and 1450 cm^{-1} are associated with the –CH bending vibrations. The characteristics peak near at 479 cm^{-1} indicates the formation of silver oxide nanoparticles.

4. Electrochemical studies

4.1 Cyclic voltammetry

The electrochemical behavior of bare SPCE and AgO/CNT/SPCE are investigated in 0.1 M PBS (pH 7.0) containing $[Fe(CN)_6]^{3-/4-}$ at a scan rate of 100 mV/s. The unmodified electrode exhibited the poor current response with no oxidation peak. After modification with silver oxide nanoparticles and carbon nanotubes, it exhibited the higher anodic peak current. The oxidation peak appeared at 807 mV with an Ipa (anodic peak current) of 1200 µA.

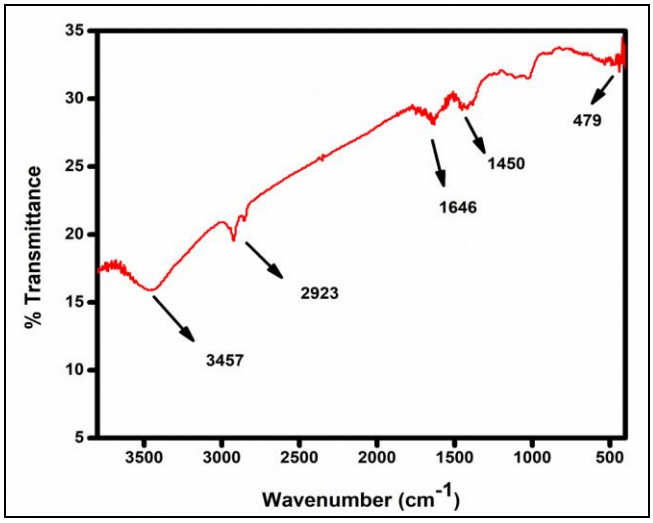

Fig 3: FTIR spectra of silver oxide NPs

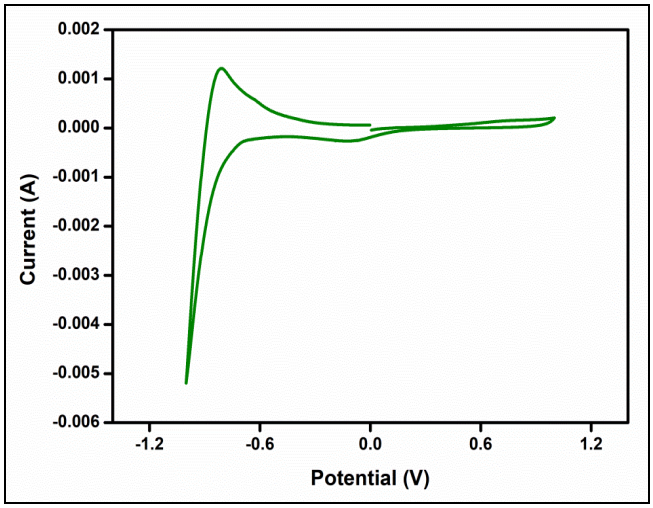

Fig 4: Cyclic Voltammograms of 0.5 mM hydrazine in 0.1 M PBS (pH 7.0) with scan rate of 100 mV/s obtained at modified SPCE

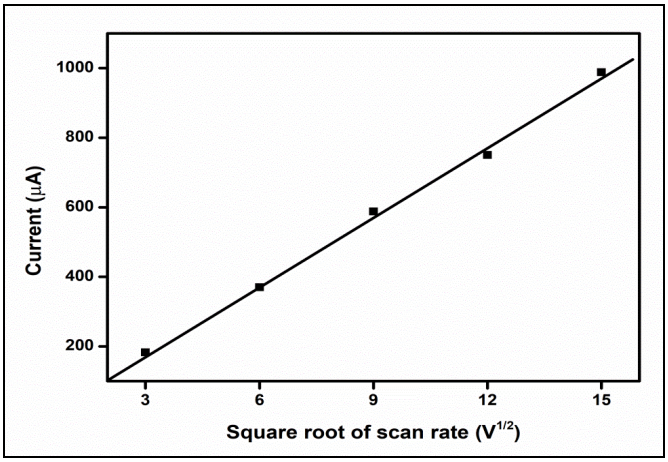

Fig 5: Different scan rates (5, 10, 20, 50, 100 mV/s) of modified electrode of 0.5 mM hydrazine in 0.1 M PBS.

In Figure 5 the scan rate experiments were also performed in 0.1 M PBS (pH 7.0) containing 0.5 mM hydrazine at the different scan rates in a range of 5, 10, 20, 50 and 100 mVs^{-1}.

The observed scan rate dependent CV graph represents that the increase in the scan rate, current values also increases which shows that the oxidation process is diffusion controlled. In figure linear relationship is observed between anodic current (Ipa) and $v^{1/2}$, which proves the diffusion-controlled kinetics. According to Randless-Sevick equation the number of electrons is 2.

4.2 Chronoamperometry

In Figure 6 (a) The fabricated sensor shows the current response increases after the addition of hydrazine and Figure 6 (b) depicts the plot between current vs hydrazine concentration. From the graph it is clear that with increase the concentration of hydrazine the value of current increases and that greatly shows the linear relationship. The sensitivity of the fabricated hydrazine sensor was 97.8 μA $\mu M^{-1}cm^{-2}$. The relationship between the hydrazine concentration and the anodic peak current showed a linear regression of *I*pa (μA) = 24.45 (μM) + 86.2 with correlation coefficient (R^2) of 0.990. The detection limit of fabricated hydrazine sensor was found to be 5μM and the response time was <3 sec.

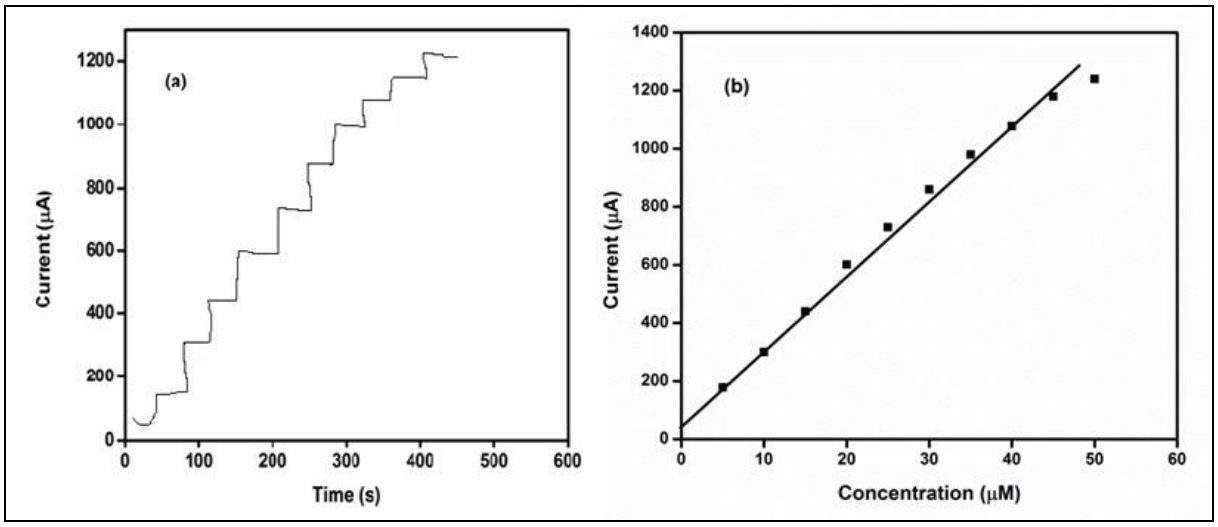

Fig 6: (a) Successive addition of hydrazine 5, 10, 15, 20, 25, 30, 35, 40, 45 and 50 μM in 0.1 M PBS (pH 7.0) solution at constant potential of 0.45 V (b) current versus concentration graph.

5. Conclusions

In the present work AgO nanoparticles were prepares by coprecipitation method. The above synthesized nanoparticles were characterized by several techniques. The electrooxidation behavior of AgO/MWCNT SPCE showed optimal response (<3s), good sensitivity (97.8 μA $\mu M^{-1}cm^{-2}$) and low detection limit 5μM and long term stability. This proposed electrode was used for rapid determination of hydrazine in clinical and pharmaceutical samples.

6. References

1. Aziz MA, Kawde AN. Gold nanoparticles-modified graphite pencil electrode for the high sensitivity detection of hydrazine, Talanta. 2013; 115:214-221.
2. Zelnick SD, Mattie DR, Stepaniak PCO. Occupational exposure to hydrazines: treatment of acute central nervous system toxicity. Aviation, Space and Environmental Medicine. 2013; 74:1285-1291.
3. Agency for Toxic Substances and Disease Registry (ATSDR). Toxicological Profile for Hydrazines, U.S. Department of Health and Human Services, Public Health Service, Atlanta, Georgia, 1997, 2-6.
4. Korfhage KM, Ravichandran K, Baldwin RP. Analytical Chemistry. 1984; 56:1514.
5. Gu X, Camden JP. Surface-enhanced raman spectroscopy-based approach for ultrasensitive and selective detection of hydrazine. Analytical Chemistry. 2015; 87:6460-6464.
6. Oh JA, Shin SH. Simple determination of hydrazine in waste water by headspace solid-phase micro extraction and gas chromatography-tandem mass spectrometry after derivatization with trifluoro pentanedione. Analytica Chimica Acta. 2017; 950: 7-63.
7. Adam KM, Kimpton H, Essen S, Davis P, Vas C, Wright

C, *et al*. Analysis of hydrazine in smokeless tobacco products by gas chromatography mass spectrometry. Chemistry Central Journal, 2015, 13-25.
8. Gionfriddo E, Naccarato A, Sindona G, Tagarelli A. Determination of hydrazine in drinking water: development and multivariate optimization of a rapid and simple solid phase microextraction-gas chromatography-triple quadrupole mass spectrometry protocol. Analytica Chimica Acta. 2014; 835:37-45.
9. Cui L, Jiang K, Liu DQ, Facchine KL. Simultaneous quantitation of trace level hydrazine and acetohydrazide in pharmaceuticals by benzaldehyde derivatization with sample 'matrix matching' followed by liquid chromatography mass spectrometry. Journal of Chromatography A. 2016; 1462:73-79.
10. Zhang HJ, Huang JS, Hou HQ, You TY. Electrochemical Detection of Hydrazine Based on Electrospun Palladium Nanoparticle/Carbon Nanofibers. Electroanalysis. 2009; 21:1869-1874.
11. Zheng L, Song JF. Ni(II)-baicalein complex modified multi-wall carbon nanotube paste electrode toward electrocatalytic oxidation of hydrazine. Talanta. 2009; 79:319-326.
12. Salimi A, Miranzadeh L, Hallaj R. Amperometric and voltammetric detection of hydrazine using glassy carbon electrodes modified with carbon nanotubes and catechol derivatives. Talanta. 2008; 75:147-156.
13. Jin R, Cao YC, Hao E, Metraux GS, Schatz GC, Mirkin CA. Controlling anisotropic nanoparticles growth through plasmon excitation. Nature. 2003; 425:487-490.
14. Navaladian S, Viswanathan B, Viswanath RP, Varadarajan TK. Thermal decomposition as route for silver nanoparticles. Nanoscale Research Letters. 2007; 2:44-48.
15. Majumder M, Chakraborty AK, Biswas B, Chowdhury A, Mallik B. Indication of formation of charge density wave in silver nanoparticles dispersed poly(methyl methacrylate) thin films. Synthetic Metals. 2011; 161:1390-1399.
16. Hosseini M, Momeni MM. Silver nanoparticles dispersed in polyaniline matrixes coated on titanium substrate as a novel electrode for electro-oxidation of hydrazine. Journal of Materials Science. 2010; 45:3304-3310.
17. Liu CJ, Burghaus U, Besenbacher F, wang ZL. Preparation and characterization of nanomaterials for sustainable energy production. ACS Nano. 2010; 4:5517-5526.
18. Tricoli A, Pratsinis SE. Dispersed nanoelectrode devices. Nature Nanotechnology. 2010; 5:54-60.
19. Ma PC, Tang BZ, Kim JK. Effect of CNT decoration with silver nanoparticles on electrical conductivity of CNT-polymer composites. Carbon, 2008; 46:1497-1505.
20. Balamurugan A, Ho KC, Chen SM. One-post synthesis of highly stable silver nanoparticles-conducting polymer nanocomposite and its catalytic application. Synthetic Metals. 2009; 159:2544-2549.
21. Lee HT, Liu YC. Catalytic electroxidation pathway for the polymerization of polypyrrole in the presence of ultrafine silver nanoparticles. Polymer. 2005; 46:10727-10732.
22. Murugan E, Jebaranjitham JN. Synthesis and characterization of silver nanoparticles supported on surface-modified poly (N-vinylimidazale) as catalysts for the reduction of 4-nitrophenol. Journal of Molecular Catalysis A: Chemical. 2012; 365:128-135.
23. Maneerung T, Tokura S, Rujiravanit R. Impregnation of silver nanoparticles into bacterial cellulose for antimicrobial wound dressing. Carbohydrate polymers. 2008; 72:43-51.
24. Vimala K, Mohan YM, Sivudu KS, Varaprasad K, Ravindra S, Reddy NN, *et al*. Fabrication of porous chitosan films impregnated with silver nanoparticles: A facile approach for superior antibacterial application. Colloids and Surfaces B: Biointerfaces. 2010; 76:248-258.